DOI: 10.1002/ejoc.200600687

Planar Chiral (Arene)chromiumcarbonyl-Substituted Propargyl Cations – A Spectroscopic and Computational Study

Astrid Netz,[a] Markus Drees,[b] Thomas Strassner,*[b] and Thomas J. J. Müller*[c]

Keywords: Alkynes / Arene complexes / DFT calculations / Cations / Chromium / Spectroscopy

Planar chiral (arene)$Cr(CO)_3$-substituted propargyl cations can be diastereoselectively generated from propargyl acetates with the use of strong Lewis acids, and they have been structurally characterized by UV/Vis and ^{13}C NMR spectroscopy. At low temperatures (<–65 °C) the s-*cis* isomer is exclusively obtained as a product of a kinetically controlled ionization. DFT studies on the structure of the propargyl cations and on the C_{ipso}–C_α bond rotation to give the thermodynamically favored s-*trans* isomer reveal that the substitution pattern at the γ-propargyl position has a stronger impact on the height of the rotational barrier than the substituent on the complexed aryl ring.

Introduction

The advent of transition metal stabilized propargyl cations has imposed a significant impact on stereoselective cationic propargylations.[1] Besides dicobalt hexacarbonyl complexed propargyl cations applied in the Nicholas reaction,[2] in the syntheses[3] of complex molecules we have demonstrated in the past years that (arene)chromiumcarbonyl-substituted propargyl cations represent complementary propargyl cation synthetic equivalents in highly stereoselective cationic propargylation reactions.[4] As for the corresponding complexed benzyl systems[5] in a stepwise ionization and nucleophilic addition to a planar chiral configurationally stable propargyl cation, a high degree of diastereoselection in the sense of retention of configuration at the propargylic stereogenic center is obtained as a consequence of a double inversion mechanism. Basic insights into the electronic structure and reactivity of (arene)chromiumcarbonyl-substituted propargyl cations were obtained by preliminary spectroscopic studies and extended Hückel calculations[4a] as well as kinetic determination of the electrophilicity[4c] of the $Cr(CO)_3$ complexed 1,3-diphenyl propargyl cation. Yet, the energetics of intramolecular dynamics such as the chromiumcarbonyl tripod and the side chain rotations, which are crucial for the conformational lock of the propargyl cation and ultimately for the diastereoselectivity of the nucleophilic addition, have remained unexplored so far. Here we report on the generation, the spectroscopic, and the computational characterization of planar chiral (arene)chromiumcarbonyl-substituted propargyl cations.

[a] ZNS Forschung, Medizinische Chemie, Abott GmbH & Co KG,
Knollstrasse, 67061 Ludwigshafen, Germany
[b] Physikalische Organische Chemie der Technischen Universität Dresden,
Bergstr. 66, 01069 Dresden, Germany
[c] Organisch-Chemisches Institut der Ruprecht-Karls-Universität Heidelberg,
Im Neuenheimer Feld 270, 69120 Heidelberg, Germany
E-mail: Thomas.J.J.Mueller@oci.uni-heidelberg.de

Generation and Spectroscopy of (Arene)-chromiumcarbonyl-Substituted Propargyl Cations

The most general access to (arene)chromiumcarbonyl-substituted propargyl cations **2** can be achieved by Lewis acid assisted extrusion of a suitable leaving group such as an acetate from corresponding propargyl acetates **1** (Scheme 1).

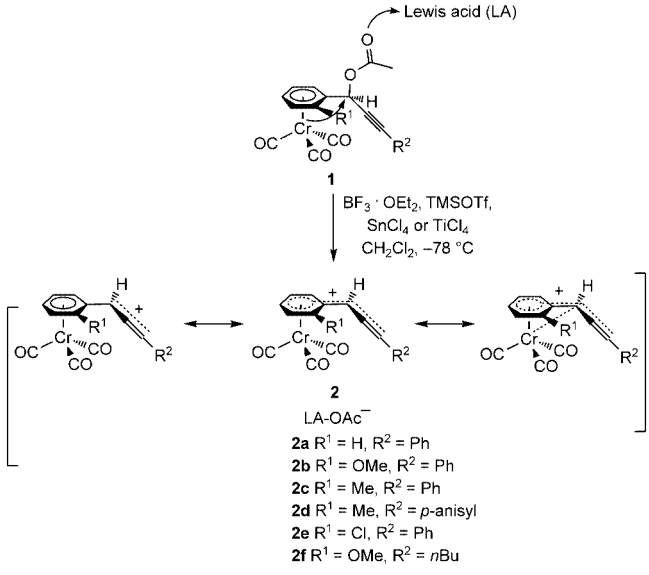

Scheme 1. Lewis acid assisted generation of (arene)$Cr(CO)_3$-substituted propargyl cations **2**.

First ionization experiments with (η^6-phenyl)$Cr(CO)_3$-substituted propargyl acetate **1a** (Scheme 1, R^1 = H, R^2 = C_6H_5) with a slight excess of boron trifluoride diethyl etherate at –78 °C in dichloromethane showed the generation of a new species accompanied by a significant color change from light yellow to deep purple within 50 min.[4a] The rate constant of the ionization of **2a** was determined as $\bar{k}_2 = (2.95 \pm 0.33)\ L\,mol^{-1}\,s^{-1}$ from a second-order rate law obtained photometrically from the increase of the long wavelength absorption band at λ_{max} = 485 nm. A short induction period is in agreement with an ionization scenario, where a preequilibrium forming Lewis acid–base adduct **3** plays a key role in the transition from acetate **1** to cation **2** (Scheme 2). In comparison, the free ligand does not at all ionize in the presence of boron trifluoride diethyl etherate under similar conditions.

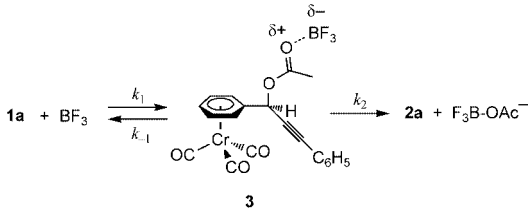

Scheme 2. Stepwise ionization by Lewis acid–base adduct **3**.

This cationic species was then identified by NMR spectroscopy to be complex substituted propargyl cation **2a**. For synthetic transformations with *ortho*-substituted η^6-phenyl complexes **1b**–**f**, stronger Lewis acids were used to accomplish complete conversion to desired propargyl cation intermediates **2b**–**f**.[4b,4d] In all cases, yellow propargyl acetates **1** give deep colored red–violet to deep blue solutions (Table 1, Figure 1) of propargyl cations **2** that are stable below –50 to –40 °C for several hours.[6]

Table 1. Longest wavelength absorption bands λ_{max} of (arene) $Cr(CO)_3$-substituted propargyl cations **2** (recorded in anhydrous dichloromethane at 207 ± 3 K).

Cation	**2a**	**2b**	**2c**	**2d**	**2e**	**2f**
λ_{max} [nm]	485	462	480	589	503	421

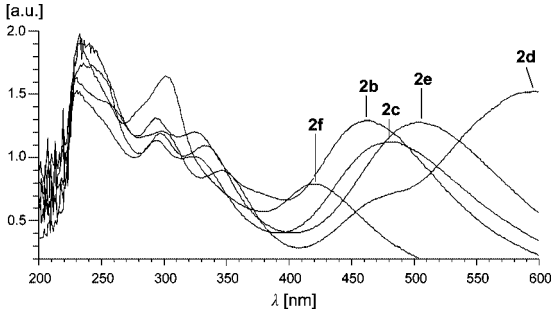

Figure 1. UV/Vis spectra of propargyl cations **2b**–**f** (recorded in dry dichloromethane at 207 ± 3 K).

The comparison of the longest wavelength absorption bands ranging from λ_{max} = 421–589 nm reveals a strong dependence on the substitution pattern of the γ-propargyl position and of the *ortho* position of the complexed benzene ring. For the γ-propargyl position, the propensity to stabilize a positive charge by resonance stabilization rather than by inductive effects is clearly reflected in lowering the energy for an electronic transition by replacing a butyl group by a phenyl or even more so by a *para*-anisyl substituent. At the *ortho* position of the complexed benzene ring, the electronic effect is opposite: with increasing acceptor character (OCH_3 < CH_3 < H < Cl) the longest wavelength maxima are shifted bathochromically. This can be interpreted on the basis that propargyl cations **2** can be regarded as organometallic push–pull chromophores[7] with the chromiumcarbonyl-complexed aryl fragment as the acceptor and the γ-propargyl substituent as the donor functionality.

Although complete ionization could be achieved at lower concentrations, the solubility of the corresponding propargyl cation is strongly dependent on the temperature and the structure. Hence, for NMR spectroscopic characterization, higher concentrations were necessary and in some cases even higher temperatures. With respect to the relative narrow temperature window (above –30 °C rapid decomposition of propargyl cations **2** was observed in all cases) and the low solubility of TMSOTf at –24 °C or the crystallization of $TiCl_4$ below –30 °C, $SnCl_4$ has turned out to be a versatile Lewis acid to achieve complete and irreversible ionization even at lower temperatures. Therefore, propargyl cation **2d** (R^1 = CH_3, R^2 = *para*-$C_6H_4OCH_3$), which is the most soluble cation, was structurally characterized by NMR spectroscopy first.

To a precooled (–70 °C) solution of acetate **1d** in CD_2Cl_2, a 15-fold excess of pure $SnCl_4$ was injected. Instantaneous measurements of ^1H, ^{13}C (Figure 2), DEPT, and CH-COSY NMR spectra at –65 °C reveal the generation of a new species with a single set of signals (Table 2). The solution of formed, diastereomerically pure propargyl cation **2d** is stable at this temperature for several hours and, thus, the unambiguous assignment of the carbon resonances of **1d** and **2d** was based in analogy to the system **1a**/**2a**[4a] and was additionally supported by the CH-COSY spectrum. Besides a significant ionization shift, most characteristically, a splitting of the resonances of the carbonyl ligands upon ionization indicates restricted rotation of the chromium carbonyl tripod as a consequence of the anchimeric stabilization[8] of the newly generated positive charge on the propargyl side chain.

Likewise, propargyl cation **2b** (R^1 = OCH_3, R^2 = Ph) was structurally characterized by ^{13}C NMR spectroscopy. As described in the previous case, the cation was generated in the NMR tube from a CD_2Cl_2 solution of propargyl acetate **1b** with $SnCl_4$ at –70 °C and transferred to the thermostatized spectrometer. Because of the increased viscosity and the accompanying signal broadening, measurements were performed above –60 °C. The carbon resonances of propargyl acetate **1b** (recorded at –87 °C) and the ionized species (recorded at –55 and –44 °C) not only revealed the generation of expected propargyl cation **2b**, but also a second propargyl cation, **2b′**, which can be identified as a diastereomer (Table 3, Figure 3).

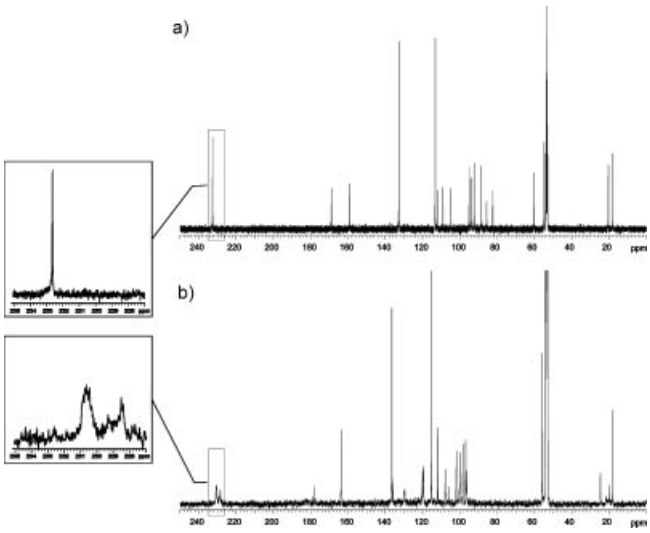

Figure 2. ^{13}C NMR spectra (recorded in CD_2Cl_2 at 203 K): a) acetate **1d** ($R^1 = CH_3$, R^2 = *para*-$C_6H_4OCH_3$) and b) propargyl cation **2d** (indentations show the carbonyl resonances).

Table 2. Assignment and ionization shifts [$\Delta\delta = \delta$(**2d**) – δ(**1d**)] of selected ^{13}C NMR signals (recorded in CD_2Cl_2, 100 MHz at 203 K).

	Acetate **1d**	Cation **2d**	Ionization shift $\Delta\delta$
Cr carbonyl	232.6	230.7	–2.1
	–	228.5	–4.1
ester carbonyl	168.9	178.0	9.1
para-*ipso*-anisyl	159.3	163.7	4.4
meta-anisyl	132.8	136.5	3.7
ortho-anisyl	113.2	115.2	2.0
ipso-anisyl	112.2	111.7	–0.5
ortho-*ipso*-η^6-aryl	109.0	107.9	–1.1
ipso-η^6-aryl	104.8	96.4	–8.4
η^6-aryl	95.1	101.9	6.8
η^6-aryl	93.7	100.1	6.4
η^6-aryl	92.4	98.5	6.1
η^6-aryl	88.4	96.9	8.5
C_γ	85.7	119.5	33.8
C_β	82.4	106.2	23.8
OCH_3 (*para*)	54.9	55.9	1.0
C_α	60.4	119.9	59.5
CH_3 (*ortho*)	18.0	17.9	–0.1
acetyl-CH_3	20.4	24.7	4.3

The ratio **2b**/**2b′** changes with increasing temperature as pointed out by the spectral development of the carbonyl resonances. Major diastereomer **2b** is converted into minor diastereomer **2b′**. Clearly, in both specimens, **2b** and **2b′**, the splitting of the carbonyl resonances indicates a restricted rotation of the chromium carbonyl tripod as a consequence of the anchimeric stabilization (Figure 4).[8] The ionization shift of the carbonyl ligands and the splitting are in good agreement with the effect of electron withdrawing substituents.[9,10]

This now implies that major s-*cis* diastereomer **2b**, generated under kinetic control, is prone to *syn–anti* isomerization of the propargyl cation side chain (Scheme 3) upon increasing the temperature to the presumably thermodynamically more stable s-*trans* cation **2b′** (vide infra).

Rotation around the C_{ipso}–C_α bond in propargyl cation **2** is very likely the cause of this dynamic phenomenon. From the difference of the averaged carbonyl resonances of **2b** and **2b′** and from the temperature regime between –55 and –44 °C, an activation barrier for the diastereomerization of 10–11 kcal mol^{-1} can be estimated. Because of the restricted solubility of specimens **2** and **2b′** at temperatures below –55 °C and their limited stability above –30 °C, it was not possible to quantify the dynamic process experimentally.

Table 3. Assignment and ionization shifts [$\Delta\delta = \delta$(**2b**) – δ(**1b**)] of selected ^{13}C NMR signals (recorded in CD_2Cl_2, 100 MHz, **1b** at 186 K, **2b** and **2b′** at 218 K and 229 K, respectively).

	Acetate **1b**	Cation, major diastereomer **2b**	Cation, minor diastereomer **2b′**	Ionization shift $\Delta\delta$[a]
Cr–*C*O	232.3	229.7	230.7	–2.6 (–1.6)
	–	229.2	230.3	–3.1 (–2.0)
	–	228.5	228.2	–3.8 (–4.1)
Ester *C*O	168.6	178.2	–	9.6
ortho-phenyl[b]	131.04	133.04	–	2.0
para-phenyl[b]	128.6	132.3	–	3.7
meta-phenyl[b]	127.8	129.0	–	1.2
ipso-phenyl[b]	120.1	120.2	119.7	0.1 (–0.4)
ortho-*ipso*-η^6-aryl	141.7	153.0	151.1	11.3 (9.4)
η^6-aryl	95.6	103.1	–	7.5
η^6-aryl	95.0	97.7	100.7	2.7 (5.7)
ipso-η^6-aryl	94.4	90.6	88.7	–3.7 (–5.9)
η^6-aryl	83.3	96.6	–	13.3
η^6-aryl	72.1	79.8	80.8	7.7 (8.7)
C_γ	84.6	118.7	119.0	34.1 (34.4)
C_β	83.7	102.6	104.8	18.9 (21.1)
C_α	57.2	106.7	107.1	49.5 (49.9)
OCH_3 (*ortho*)	55.7	58.0	58.3	2.3 (2.6)
acetyl-CH_3	20.2	24.8	–	4.6

[a] Ionization shift of the minor diastereomer in parentheses. [b] Assigned according to the precedence **1a**/**2a**.[4a]

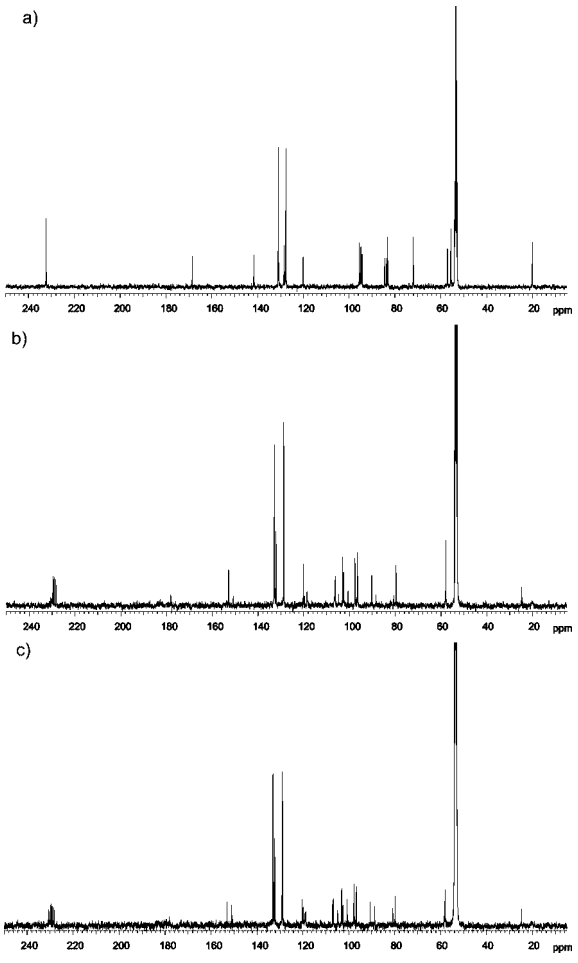

Figure 3. ^{13}C NMR spectra (recorded in CD_2Cl_2): a) acetate **1b** (R^1 = OCH_3, R^2 = C_6H_5) at 186 K, b) propargyl cation **2b** at 218 K, and c) the mixture of diastereomeric propargyl cations **2b** and **2b′** at 229 K.

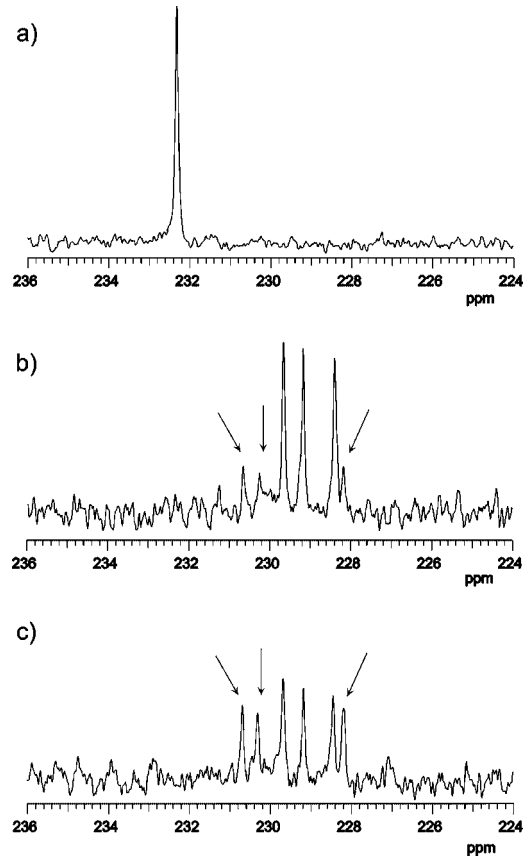

Figure 4. Carbonyl resonances in the ^{13}C NMR spectra (recorded in CD_2Cl_2): a) acetate **1b** (R^1 = OCH_3, R^2 = C_6H_5) at 186 K, b) propargyl cation **2b** at 218 K, and c) the mixture of diastereomeric propargyl cations **2b** and **2b′** (marked by arrows) at 229 K.

Computational Studies on (Arene)-chromiumcarbonyl-Substituted Propargyl Cations

The lack of an experimental option to determine the barrier of the rotation around the C_{ipso}–C_α bond in propargyl cation **2** as the origin of the observed diastereomer distribution and stereomutation in the one-step ionization trapping protocol[4d] in nucleophilic trapping reactions prompted us to quantitatively study the *syn–anti* isomerization by computational methods. Therefore, we set out to calculate energies[11] for cations **2b**–**d**, **2g** (R^1 = Me, R^2 = $SiMe_3$), and **2h** (R^1 = Me, R^2 = *n*Bu) by using Gaussian-03[12] and by applying the hybrid DFT[13] method B3LYP[14] with a 6-31G* basis set.[15] Inspection of the conformational energies with frozen dihedral angles reveals that the provisional rotational barrier for aryl substituents in the γ-propargyl positions is significantly lower than that of either alkyl or silyl substituents (Figure 5). Interestingly, it becomes evident that for aromatic γ-substituents the rotation *endo* with respect to the chromiumcarbonyl tripod is energetically favored.

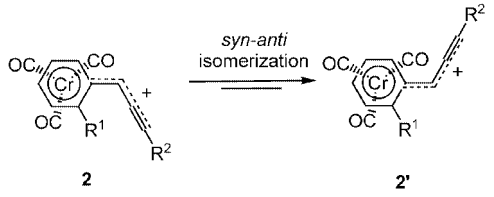

Scheme 3. *syn–anti* isomerism of propargyl cations **2**/**2′**.

The s-*cis* propargyl cations **2** and the s-*trans* propargyl cations **2′** (see for example Figure 6: **2g** and **2g′**) were optimized. As expected, the s-*cis* diastereomer is generally 2.0–2.9 kcal mol^{-1} higher in energy than the s-*trans* isomer (Table 4).

We compared the C_{ipso}–C_α bond lengths and the deviation of the dihedral angle C_α–C_{ipso}–C_{ortho}–H_{ortho} (see Figure 6) of the substituents towards the η^6-coordinated aryl system. The C–C distances are calculated to be 1.42 ± 0.01 Å for all systems. Within that narrow margin, those with R^2 = aryl are calculated to be longer than those with non-aromatic R^2 groups. The difference between the aryl and the other R^2 substituents becomes even more obvious in the deviation from the planar geometry. All compounds with R^2 = aryl (**2b**–**2d** and isomers) show smaller deviations of 7 to 13 °, while in **2g** (R^2 = $SiMe_3$) and **2h** (R^2

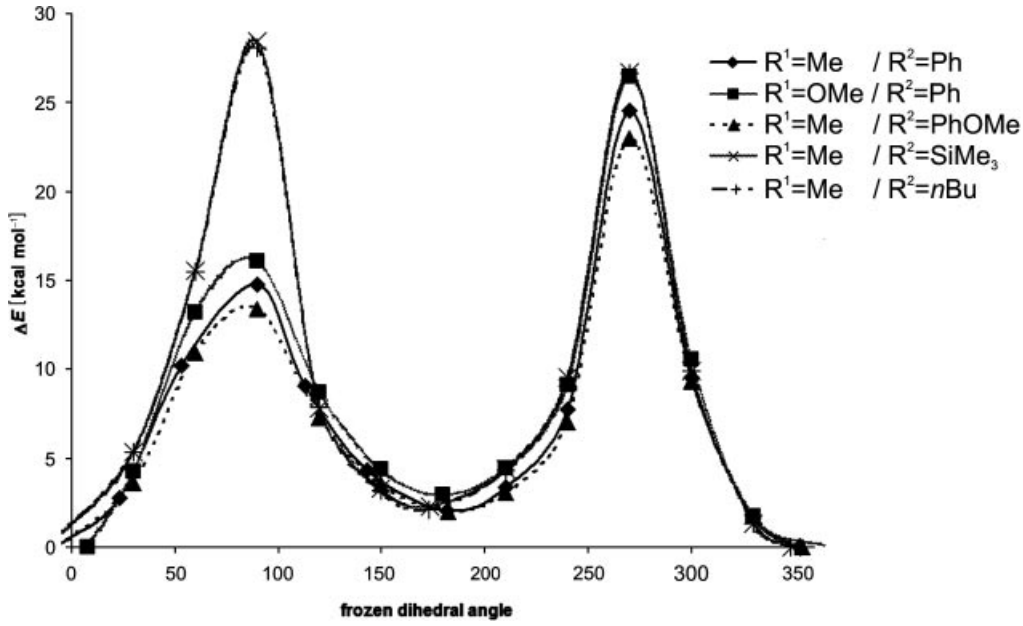

Figure 5. Calculated conformational energies at frozen dihedral angles for rotation around the C_{ipso}–C_α bond in propargyl cations **2b**–**d**, **2g** (R^1 = Me, R^2 = $SiMe_3$), and **2h** (R^1 = Me, R^2 = *n*Bu.

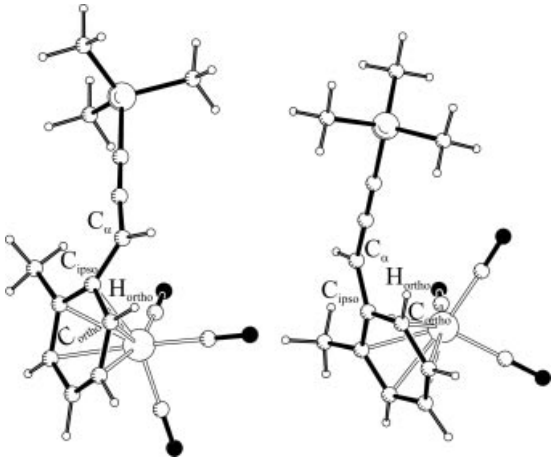

Figure 6. Calculated isomers **2g** (left) and **2g′** (right).

Table 4. Computed gas phase energies (in [kcal mol^{-1}]) and solvent calculations (in [kcal mol^{-1}]) of conformers **2** and **2′** and of the transition states for C_{ipso}–C_α bond rotation.

	$\Delta H_{2-2'}$	$\Delta G_{2-2'}$	$\Delta E_{2-2'(solv)}$	$\Delta H^{\ddagger}_{2\rightarrow2'}$	$\Delta G^{\ddagger}_{2\rightarrow2'}$	$\Delta E^{\ddagger}_{2\rightarrow2'(solv)}$
2b	+2.9	+2.7	+2.0[g]	+19.4[a,f]	+19.3[a,f]	+18,4[f,g]
2c	+2.1	+2.3	+1.0[g]	+19.4[b]	+20.7[b]	+18.9[g]
2d	+2.0	+2.2	+0.8[g]	+16.1[c]	+17.7[c]	+14.7[g]
2g	+2.3	+2.2	+0.8[g]	+25.8[d]	+26.3[d]	+26.9[g]
2h	+2.1	+1.9	–0.3[g]	+25.5[e]	+25.7[e]	+25.4[g]

[a] Imaginary frequencies that verify transition states: i221 cm^{-1}. [b] i173 cm^{-1}. [c] i112 cm^{-1}. [d] i314 cm^{-1}. [e] i336 cm^{-1}. [f] Triplet multiplicity. [g] Solvent single-point calculations on gas-phase optimized geometries.

= *n*Bu) the corresponding dihedral angle increases to around 20 °. Earlier, extended Hückel calculations of other aryl–chromium complexes by McGlinchey[5e] reported deviations of 22 °, and DFT studies by Koch and Schmalz[13a] show angles of inclination of even 37 ° out of the planarity of the η^6-coordinated aryl system.

Least energy transition states **4** are represented by *endo* orientation of the propargyl side chain, which is in agreement with an almost orthogonal arrangement of the propargyl cation and the η^6 complexed aryl ring (Scheme 3, Figure 7). Therefore, the heights of the rotational barriers calculated as $\Delta H^{\ddagger}$ lie between 16 and 26 kcal mol^{-1}. Although, the calculated barriers are significantly higher than the experimentally estimated activation energies for the diastereomerization and deviate by 6–16 kcal mol^{-1}, the trends are self-consistent, where stronger electron donating substituents on the complexed arene ring cause a stronger restriction of the rotation than placing them in the γ-propargyl position. This trend is also observed in the diastereoselectivities of the nucleophilic trapping reactions.[4d]

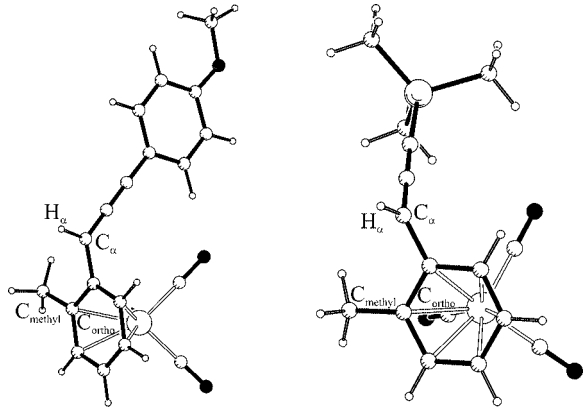

Figure 7. Calculated transition states **4d** (left) and **4g** (right).

In the transition state structures, the C_{ipso}–C_α bond lengths are elongated in comparison to the corresponding cationic ground state geometries. Again the nature of the substituent R^2 leads to a significant difference. For transition states **4g** (R^2 = $SiMe_3$) and **4h** (R^2 = *n*Bu) the C_{ipso}–C_α bond length is shorter (1.468 Å) compared to the aryl substituents in **4b**–**4d**, where this bond length increases to 1.476–1.480 Å.

The deviation in the coplanarity of the C_{ipso}–C_α bond from the planar aromatic system of the η^6-coordinated aryl ring is smaller than the cationic ground states. Dihedral angles of 5–10 ° deviation with respect to the corresponding cationic ground state are calculated. The propargyl C_α–H_α bond is almost orthogonal to the aryl chromium complex with torsion angles (H_α–C_α–C_{ortho1}–C_{Methyl}, see Figure 7) of 78 to 82 ° in all calculated transition states.

In the case of transition states **4b** and **4d** we also checked higher spin states. For ground states **2b/2b′** and **2d/2d′**, the corresponding triplet spin states are disfavored by 6–10 kcal mol^{-1}. They are all located on the singlet potential energy surface. The "two-state-reactivity" concept proposed by Schwarz et al.[16] allows selected first-row transition metals to react on a different hypersurface, for example by a higher multiplicity exclusively for the transition state. For transition state **4d** (R^1 = Me, R^2 = *para*-anisyl), the triplet state remains unfavorable although the energy difference of the two spin states is calculated to be only 3 kcal mol^{-1}.

But a two-state-reactivity is indeed proposed for transition state **4b** (R^1 = OMe, R^2 = phenyl). For the singlet state, a free energy of 22.6 kcal mol^{-1} is calculated, the corresponding triplet state is about 3.3 kcal mol^{-1} lower (ΔG). Therefore, it is in that case possible that the two singlet state isomers are connected via a triplet transition state. Because of the oxygen function in R^1 it seems that the necessary biradical character is favored in this transition state. There are only small structural differences between the singlet and the triplet state of transition state **4b**. The distance of the OMe group (R^1) to the chromium–aryl complex is larger in the higher spin state (triplet: 1.34 Å, singlet: 1.32 Å), and also the distance of the carbonyl ligands to the chromium center changes. In the singlet state, the average distance of the three ligands is 1.87 Å, while in the triplet state their mean value is 1.91 Å.

To probe for a possible solvent effect of DCM, single point calculations using the PCM method[17] were conducted on the optimized gas-phase structures (Table 4). For all systems the effect is only small. The energy difference between the *syn* and *anti* isomers becomes smaller, and in the case of **2h′** the *s-trans* isomer in solution is even lower in energy than its s-*cis* isomer, **2h**. The transition states show a clear dependence of the solvent effects on the substituent R^2. For aryl groups, the rotational barrier decreases by 1–3 kcal mol^{-1}, whereas the silyl and *n*Bu groups show only a small (**4h**) or even an opposed influence (**4g**) of the solvent.

In the case of the one-state-reactivity system **2d**–**4d**–**2d′** (R^1 = Me, R^2 = *para*-anisyl) the solvent effects were studied in more detail by reoptimizing the three stationary points by using the PCM method.[17] By comparing the single-point energies on the gas-phase geometries to the energies calculated for the structures optimized in the solvent, it becomes obvious that there is no significant change in the geometries of the two cations and the transition state. For the ground state, the calculated energies are identical, whereas for the transition state, the solvent corrections of the single-point calculation (+14.7 kcal/mol) overestimate the solvent effect when compared with +15.4 kcal mol^{-1} for the reoptimized structure.

As a consequence for further methodological applications, the use of alkyl or silyl substituents in the γ-propargyl position not only diminishes the rotation around the C_{ipso}–C_α bond in propargyl cations **2**, but they also preserve the stereochemical integrity during the ionization–nucleophilic trapping sequences. Therefore, these types of propargyl cations should be most favorable for stereoselective syntheses of complex molecules (Scheme 4).

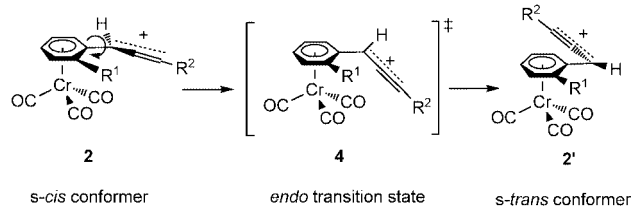

Scheme 4. C_{ipso}–C_α bond rotation as the origin of the *syn–anti* isomerism of propargyl cations **2**/**2′**.

In conclusion, we have demonstrated that planar chiral (arene)$Cr(CO)_3$-substituted propargyl cations can be diastereoselectively generated from propargyl acetates with strong Lewis acids at a reasonable rate. UV/Vis and ^{13}C NMR spectroscopy have been successfully applied to unambiguously characterize these cationic species. At low temperatures (<–65 °C), the s-*cis* isomer is exclusively obtained as a product of kinetically controlled ionization in agreement with a chromiumcarbonyl-assisted neighboring-group participation in an *anti*-periplanar acetate extrusion. The origin of epimerization at the propargylic center is obviously a C_{ipso}–C_α bond rotation that causes *syn–anti* isomerism towards the thermodynamically more favored s-*trans* propargyl cation isomer. Computational studies on the C_{ipso}–C_α bond rotation reveal that the substitution pattern at the γ-propargyl position has a stronger impact on the height of the rotational barrier than the substituent on the complexed aryl ring.

Experimental and Computational Section

All reactions involving tricarbonylchromium complexes were carried out in flame-dried Schlenk flasks under a nitrogen atmosphere and by using septum and syringe techniques. Solvents were dried and distilled according to standard procedures.[18] ^1H- and ^{13}C NMR spectra were recoded with a Bruker ARX 300 or a Varian VXR 400S instrument. The assignments of quaternary C, CH, CH_2, and CH_3 have been made by using DEPT spectra. UV/Vis spectra were recorded with a Perkin–Elmer Lambda 16 or J&M TIDAS (transputer integrated diodes array spectrometer) instru-

ment with a Hellma low temperature quartz probe and J&M Spektralys program 1.5.5 for evaluation, Schölly UV spectrometer KGS III Intraphotometer.

Generation of the Planar Chiral (arene)$Cr(CO)_3$-Substituted Propargyl Cations

For UV/Vis Spectroscopic Studies: Standard solutions of propargyl acetates **1** (10^{-3} M in dichloromethane) were prepared under rigorous exclusion of moisture. A well-defined volume of the standard solution was injected into a measuring flask containing precooled (–65 °C) and dry dichloromethane (for experimental details see Table 5). After recording the spectrum of acetate **1**, a precooled Lewis acid (BF_3·OEt_2 or TMSOTf) was added by a thermostatized syringe in a tenfold excess at –65 °C. After stirring for 50 min at this temperature, the spectrum of cation **2** was recorded.

Table 5. Experimental details for ionization of propargyl acetates **1** (UV/Vis studies).

Entry	Temperature [°C]	Propargyl acetate **1** [mol L^{-1}]	Lewis acid [mol L^{-1}]
1	–64.2	1.54×10^{-4} of **1b**	2.61×10^{-3} of BF_3·OEt_2
2	–65.4	1.45×10^{-4} of **1c**	1.41×10^{-3} of TMSOTf
3	–69.1	1.44×10^{-4} of **1d**	3.12×10^{-3} of TMSOTf
4	–66.0	1.98×10^{-4} of **1e**	7.02×10^{-3} of TMSOTf
5	–65.7	1.74×10^{-4} of **1f**	7.05×10^{-3} of TMSOTf

For ^{13}C NMR Spectroscopic Studies: Propargyl acetates **1** were placed in an NMR tube under an argon atmosphere and sealed with a septum. To these NMR tubes, anhydrous deuterated dichloromethane was added (0.3–0.6 mL) (for experimental details, see Table 6). The spectra of acetates **1** were then recorded at –87 and –70 °C, respectively. The NMR tubes were then cooled in Dewar vessel to –70 °C (dry ice/acetone). An excess of a precooled Lewis acid (as a solution in deuterated dichloromethane) was injected by a thermostatized cannula to the bottom of the NMR tubes. Cooling was maintained until the tube was quickly placed into the thermostatized conduit of the NMR apparatus. After 2–5 min of shimming, the measurements were started.

Table 6. Experimental details for ionization of the propargyl acetates **1** (^{13}C NMR studies).

Entry	Temperature [°C]	Propargyl acetate **1**	Lewis acid
1	–55 and –44	32 mg (0.8 mmol) of **1c**	0.18 mL (0.12 mmol) of 0.68 M $SnCl_4$
2	–65	9 mg (0.9 mmol) of **1d**	0.20 mL (0.15 mmol) of 0.77 M $SnCl_4$

Computational Studies: All calculations were performed with the software package GAUSSIAN-03[12] by using the density functional/Hartree–Fock hybrid model Becke3LYP[14] and the split valence double-ζ (DZ) basis set 6-31G(d).[15] No symmetry or internal coordinate constraints were applied during optimizations except for the calculations leading to the results in Figure 5. All reported intermediates were verified as true minima by the absence of negative eigenvalues in the vibrational frequency analysis. Transition-state structures were located by using the Berny algorithm[19] until the Hessian matrix had only one imaginary eigenvalue. The identity of all transition states was confirmed by IRC calculations and by animating the negative eigenvector coordinate with MOLDEN[20] and GaussView.[21]

Approximate free energies (ΔG) and enthalpies (ΔH) were obtained through thermochemical analysis of frequency calculations by using the thermal correction to Gibbs free energy as reported by GAUSSIAN-03. This takes into account zero-point effects, thermal enthalpy corrections and entropy. All energies reported in this paper, unless otherwise noted, are free energies or enthalpies at 298 K with the use of unscaled frequencies. All transition states are maxima on the electronic potential energy surface (PES), which may not correspond to maxima on the free energy surface. Solvation corrections were applied by using the PCM model[17] as implemented in GAUSSIAN-03. Table 4 includes single-point calculations while for **2d**–**4d**–**2d′** the stationary points were also reoptimized in solution.

Acknowledgments

The financial support of the Fonds der Chemischen Industrie (scholarship to A. N.) and Deutsche Forschungsgemeinschaft is gratefully acknowledged. We cordially thank Dr. David S. Stephenson, LMU München, for valuable discussions and his helpful instructions for the NMR spectrometer. M. D. and T. S. thank the center of high-performance computing (ZIH) of the TU Dresden for providing computing time on their computer systems.

[1] For a recent review on stereoselective cationic propargylations, see, for example: T. J. J. Müller, *Eur. J. Org. Chem.* **2001**, 2021–2033.

[2] For excellent reviews see, for example: a) G. G. Melikyan, K. M. Nicholas in *Modern Acetylene Chemistry* (Eds.: P. J. Stang, F. Diederich), VCH, Weinheim, **1995**, p. 118; b) A. J. M. Caffyn, K. M. Nicholas in *Comprehensive Organometallic Chemistry II* (Eds.: E. W. Abel, F. G. A. Stone, G. Wilkinson), Pergamon, Oxford, **1995**, vol. 12, p. 685.

[3] a) K. C. Nicolaou, W. M. Dai, *Angew. Chem.* **1991**, *103*, 1453–1481; *Angew. Chem. Int. Ed. Engl.* **1991**, *30*, 1387–1416; b) P. Magnus, T. Pitterna, *J. Chem. Soc., Chem. Commun.* **1991**, 541–543; c) P. Magnus, *Tetrahedron* **1994**, *50*, 1397–1418.

[4] a) T. J. J. Müller, A. Netz, *Organometallics* **1998**, *17*, 3609–3614; b) T. J. J. Müller, A. Netz, *Tetrahedron Lett.* **1999**, *40*, 3145–3148; c) A. Netz, T. J. J. Müller, *Tetrahedron* **2000**, *56*, 4149–4155; d) A. Netz, K. Polborn, T. J. J. Müller, *J. Am. Chem. Soc.* **2001**, *123*, 3441–3453; e) A. Netz, K. Polborn, H. Nöth, T. J. J. Müller, *Eur. J. Org. Chem.* **2005**, 1823–1833.

[5] a) D. K. Wells, W. S. Trahanovsky, *J. Am. Chem. Soc.* **1969**, *91*, 5870–5872; b) G. A. Olah, S. H. Yu, *J. Org. Chem.* **1976**, *41*, 1694–1697; c) D. Seyferth, S. Merola, C. S. Eschbach, *J. Am. Chem. Soc.* **1978**, *100*, 4124–4131; d) D. W. Clack, L. A. P. Kane-Maguire, *J. Organomet. Chem.* **1978**, *145*, 201–206; e) P. A. Downton, B. G. Sayer, M. J. McGlinchey, *Organometallics* **1992**, *11*, 3281–3286.

[6] For system **2f**, the influence of the counterion on the UV/Vis spectrum was studied upon ionizing **1f** with TMSOTf, $SnCl_4$, and $TiCl_4$. The obtained spectra were identical; however, the rate of complete ionization of a 10^{-4} M solution varied from 1 to 13 min depending on the strength of the Lewis acid used.

[7] N. J. Long, *Angew. Chem.* **1995**, *107*, 37–56; *Angew. Chem. Int. Ed. Engl.* **1995**, *34*, 6–20.

[8] For reviews on the generation of transition metal complex stabilized carbenium ions by neighboring group participation, see, for example: a) L. Haynes, R. Pettit in *Carbonium Ions* (Eds.: G. A. Olah, P. v. R. Schleyer), Wiley, New York, **1975**, vol. 5; b) W. E. Watts in *Comprehensive Organometallic Chemistry* (Eds.: G. Wilkinson, F. G. A. Stone, E. W. Abel), Pergamon, Oxford, **1982**, vol. 8, ch. 59, p. 1051; c) A. Solladié-Cavallo, *Polyhedron* **1985**, *4*, 901–927; d) G. Jaouen, *Pure Appl. Chem.* **1986**, *58*, 597–616; e) K. M. Nicholas, *Acc. Chem. Res.* **1987**, *20*, 207–214; f) for stabilization of positive charge in benzylic positions by chromium carbonyl fragments, see, for example: S. G. Davies, T. J. Donohoe, *Synlett* **1993**, 323–332.

[9] S. Top, G. Jaouen, *J. Org. Chem.* **1981**, *46*, 78–82.
[10] a) O. L. Carter, A. T. McPhail, G. A. Sim, *J. Chem. Soc. A* **1967**, 228–236; b) T. A. Albright, P. Hofmann, R. Hoffmann, *J. Am. Chem. Soc.* **1977**, *99*, 7546–7557; c) M. J. McGlinchey, *Adv. Organomet. Chem.* **1992**, *34*, 285–325.
[11] Thermochemical data were determined at 298.15 K unless stated otherwise.
[12] M. J. Frisch, G. W. Trucks, H. B. Schlegel, G. E. Scuseria, M. A. Robb, J. R. Cheeseman, J. A. Montgomery Jr, T. Vreven, K. N. Kudin, J. C. Burant, J. M. Millam, S. S. Iyengar, J. Tomasi, V. Barone, B. Mennucci, M. Cossi, G. Scalmani, N. Rega, G. A. Petersson, H. Nakatsuji, M. Hada, M. Ehara, K. Toyota, R. Fukuda, J. Hasegawa, M. Ishida, T. Nakajima, Y. Honda, O. Kitao, H. Nakai, M. Klene, X. Li, J. E. Knox, H. P. Hratchian, J. B. Cross, V. Bakken, C. Adamo, J. Jaramillo, R. Gomperts, R. E. Stratmann, O. Yazyev, A. J. Austin, R. Cammi, C. Pomelli, J. W. Ochterski, P. Y. Ayala, K. Morokuma, G. A. Voth, P. Salvador, J. J. Dannenberg, V. G. Zakrzewski, S. Dapprich, A. D. Daniels, M. C. Strain, O. Farkas, D. K. Malick, A. D. Rabuck, K. Raghavachari, J. B. Foresman, J. V. Ortiz, Q. Cui, A. G. Baboul, S. Clifford, J. Cioslowski, B. B. Stefanov, G. Liu, A. Liashenko, P. Piskorz, I. Komaromi, R. L. Martin, D. J. Fox, T. Keith, M. A. Al-Laham, C. Y. Peng, A. Nanayakkara, M. Challacombe, P. M. W. Gill, B. Johnson, W. Chen, M. W. Wong, C. Gonzalez, J. A. Pople, *Gaussian 03*, Revision C.02, Gaussian, Inc., Wallingford, CT, **2004**.
[13] For computational studies on chromiumcarbonyl complexes on the DFT level of theory, see, for example: a) A. Pfletschinger, T. K. Dargel, J. W. Bats, H.-G. Schmalz, W. Koch, *Chem. Eur. J.* **1999**, *5*, 537–545; b) C. A. Merlic, J. C. Walsh, D. J. Tantillo, K. N. Houk, *J. Am. Chem. Soc.* **1999**, *121*, 3596–3606.
[14] a) C. Lee, W. Yang, R. G. Parr, *Phys. Rev. B: Condens. Matter* **1988**, *37*, 785–789; b) S. H. Vosko, L. Wilk, M. Nusair, *Can. J. Phys.* **1980**, *58*, 1200–1211; c) A. D. Becke, *J. Chem. Phys.* **1993**, *98*, 5648–5652; d) P. J. D. Stephens, F. J. Devlin, C. F. Chabalowski, M. J. Frisch, *J. Phys. Chem.* **1994**, *98*, 11623–11627.
[15] a) P. C. Hariharan, J. A. Pople, *Theoret. Chim. Acta* **1973**, *28*, 213–222; b) M. M. Mancl, W. J. Petro, W. J. Hehre, J. S. Binkley, M. S. Gordon, D. J. DeFree, J. A. Pople, *J. Chem. Phys.* **1982**, *77*, 3654–3665; c) V. Rassolov, J. A. Pople, M. Ratner, T. L. Windus, *J. Chem. Phys.* **1998**, *109*, 1223–1229.
[16] D. Schroeder, S. Shaik, H. Schwarz, *Acc. Chem. Res.* **2000**, *33*, 139–145.
[17] a) S. Miertus, E. Scrocco, J. Tomasi, *Chem. Phys.* **1981**, *55*, 117–129; b) B. Mennucci, J. Tomasi, *J. Chem. Phys.* **1997**, *106*, 5151–5158; c) R. Cammi, B. Mennucci, J. Tomasi, *J. Phys. Chem. A* **2000**, *104*, 5631–5637; d) M. Cossi, G. Scalmani, N. Rega, V. Barone, *J. Chem. Phys.* **2002**, *117*, 43–54.
[18] H. G. O. Becker, R. Beckert, G. Domschke, E. Fanghänel, W. D. Habicher, P. Metz, D. Pavel, K. Schwetlick (Eds.), *Organikum*, 21st ed., Wiley-VCH, Weinheim, **2001**.
[19] H. B. Schlegel, *J. Comput. Chem.* **1982**, *3*, 214–218.
[20] G. Schaftenaar, J. H. Noordik, *J. Comput.-Aided Mol. Design* **2000**, *14*, 123–134.
[21] GaussView, Version 3.09, R. Dennington II, T. Keith, J. Millam, K. Eppinnett, W. L. Hovell, R. Gilliland; Semichem, Inc., Shawnee Mission, KS, **2003**.

Received: August 7, 2006
Published Online: November 21, 2006

